Title
Study of gas hydrates in the deep-sea Gulf of Mexico from seismic data

Journal
SEG Technical Program Expanded Abstracts, 22(1)

ISSN
1052-3812

Authors
Cassassuce, Florence
Rector, James
Hoversten, Mike

Publication Date
2003

DOI
10.1190/1.1817941

Peer reviewed

Study of gas hydrates in the deep-sea Gulf of Mexico from seismic data

Florence Cassassuce[1], James W. Rector[1], G. Michael Hoversten[2]

[1] UC Berkeley
[2] Lawrence Berkeley National Laboratory

DOI: 10.1190/1.1729223

Summary

Historically, the presence of methane hydrate has been inferred on the basis of bottom simulating reflectors (BSRs), which are believed to mark the phase boundary between hydrate and the probable underlying free gas zone. However, in the Gulf of Mexico, laterally continuous BSRs have not been observed. The presence of laterally discontinuous vertical migration pathways may be one possible reason for the absence of BSRs in the Gulf of Mexico. To investigate this hypothesis, we use the data from a seismic survey conducted in water depth of about 1500 m. We perform a three parameter AVO inversion on the portion of the 2D seismic line in the vicinity of a salt tongue where gas hydrate accumulations may be concentrated. We identify a possible hydrate accumulation that extends 3000 m laterally from the salt flank. The hydrate reservoir is estimated to be 40 m in thickness and overlays a 20 m transition layer between hydrate and free gas. The total volume of methane gas in the reservoir is in the range of 126 to 252 billion cubic feet.

Introduction

In the Gulf of Mexico, gas hydrates have been found in a number of surface expressions and analysis of piston cores. However, the classic seismic detection method - looking for semi-continuous Bottom Simulating Reflectors (BSRs) - has not been successful in revealing hydrate reservoirs.

Sassen and Milkov (2001) postulate that, in the Gulf of Mexico, gas hydrate accumulations are concentrated along the rims of salt-withdrawal basins and over salt-ridges where there is often intense fracturing and faulting. Fractures may act as conduits for the focused upward expulsion of fluids and methane gas. This is referred to as channeled flux (Xu and Ruppel, 1999), in which a few preferred pathways transport the majority of the fluid. Figure 1 illustrates this scenario by presenting a modeled distribution of gas hydrates within the gas hydrate stability zone (GHSZ) at the Mississippi Canyon 853 site. As a result, we would not expect to see a laterally continuous BSR such as is observed in tectonically less active areas such as Blake Ridge.

We use the data from a 2-D seismic survey conducted in Mississippi Canyon Block 383 to search for potential hydrate reflections within the hydrate stability zone in the vicinity of faults (i.e. near the salt dome).

The gas hydrate stability zone is estimated by using the empirical equation proposed by Brown et al. (1996). On the stacked section two reflection events are identified approximately at the base of the GHSZ. To analyze these reflections, a three parameter AVO inversion is performed on multiple cdp's over an angle range from 0-35 degrees. Finally an estimate of the gas hydrate concentration and the total volume of methane gas are given based on the elastic model of Dvorkin et al. (2000).

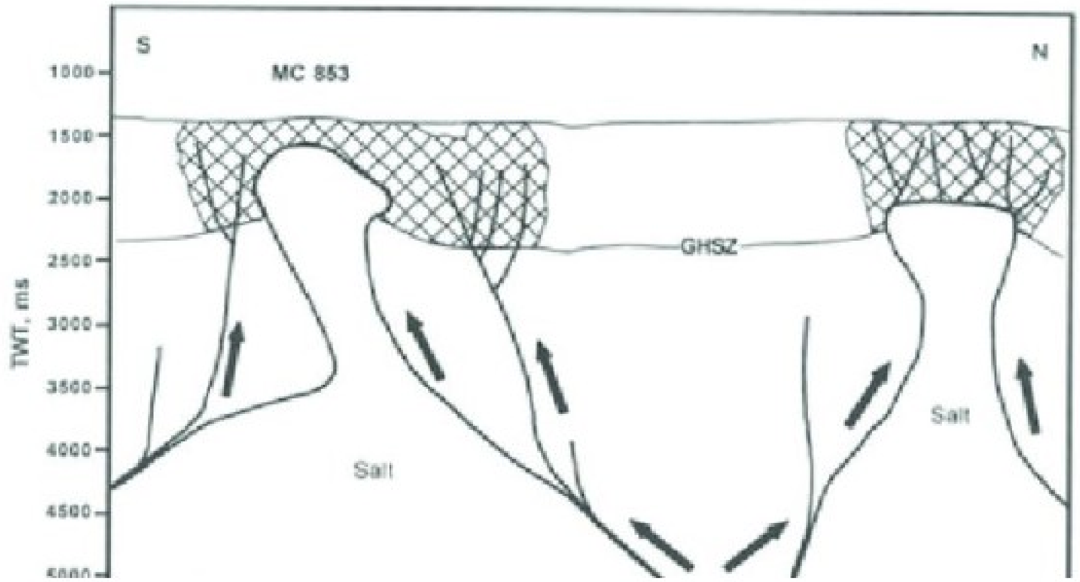

Figure 1: Sketch showing hypothesized subsurface distribution of gas hydrate at Mississippi Canyon Block 853 (hatched areas). (from Sassen and Milkov, 2001). The base of gas hydrate stability zone (GHSZ) is a line connecting the two salt domes.

Prediction of hydrate stability zone

To estimate the Pressure-Temperature (P-T) conditions for the boundary of the gas hydrate stability field. Dickens and Quinby-Hunt (1994) were the first investigators to make measurements of methane hydrate stability in seawater, Brown et al. (1996) fit the data of Dickens and Quinby-Hunt to a second order polynomial and obtained the following equation:

(1) $$1/T = 3.83\times10^{-3} - 4.09\times10^{-4} \log_{10} P + 8.64\times10^{-5} (\log_{10} P)^2$$

The ocean bottom depth for our Mississippi Canyon site is 1500 m. A value of 18.3° C/1000 m was assumed for the Gulf of Mexico temperature gradient below OB and a variation of ±0.915° C/1000 m from this value is represented on the adjacent curves. The methane hydrate stability zone is found between the ocean bottom and 350±20 m, given by the intersection of the two curves.

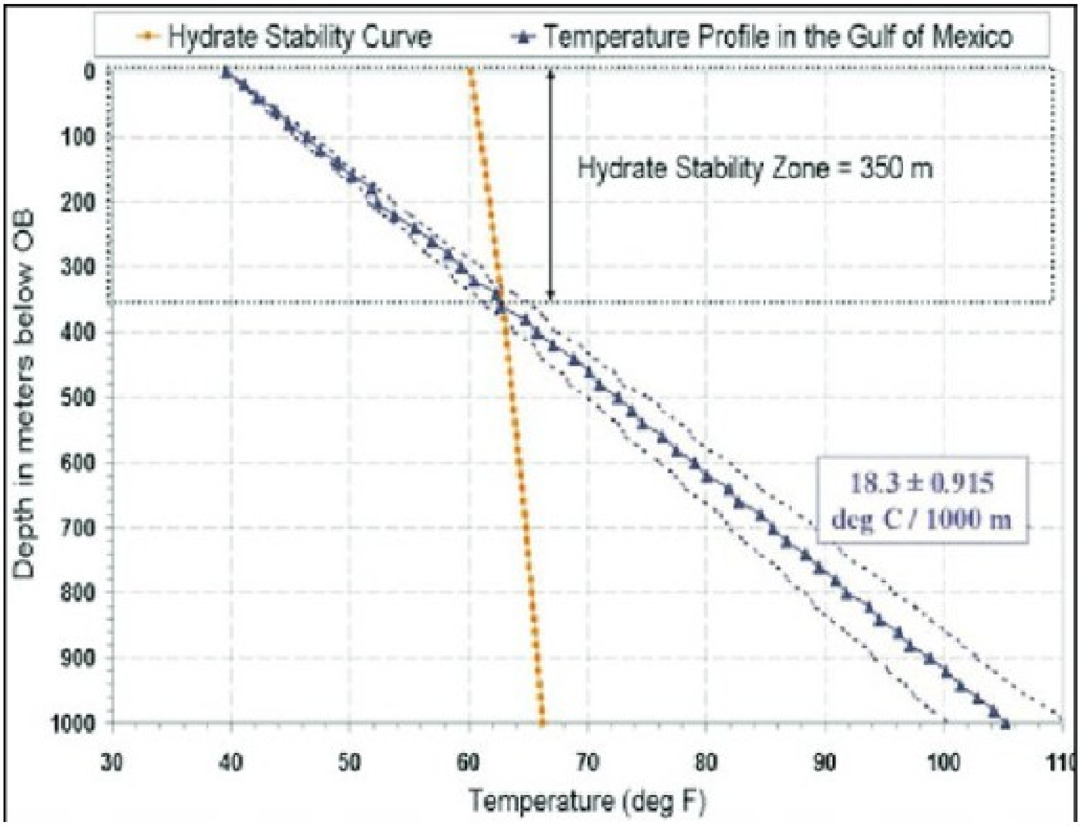

Figure 2: Prediction of Methane Hydrate Stability Zone

Data acquisition and processing

Data were acquired with 4 ms sampling rate, 16s total recording time and maximum offset of 3000 meters. The recorded amplitudes are calibrated to true reflection coefficients using the water bottom reflection. The water bottom reflection coefficient is estimated to be 0.32 corresponding to the following velocity and density changes at OB:

Vs_{OB-} = 0 m/s	Vs_{OB+} = 100 m/s
Vp_{OB-} = 1500 m/s	Vp_{OB+} = 1650 m/s
ρ_{OB-} = 1035 kg/m3	ρ_{OB+} = 1800 kg/m3

Figure 3 shows the stacked section in the vicinity of a salt tongue. The section was vertically stretched to depth using a velocity model that was first derived from the semblance velocity spectrum analysis and then conformed to the structure seen on the seismic section. A bright event is located at 2000 m (2460 ms) which is the predicted depth of the base of methane hydrate stability zone (i.e. the BSR). The event appears to be continuous from CDP 800 to the flank of the salt dome at CDP 1100., which is consistent with the hypothesized subsurface distribution of gas hydrates presented in Figure 1.

Method

The elastic parameters may be estimated using a linearized approximation of the Zoeppritz equation (Aki and Richards,1980)

$$R(\theta) = \frac{1}{2}(1 - 4\gamma^2 \sin^2\theta)\frac{\Delta\rho}{\rho} + \frac{1}{2}\frac{\Delta\alpha}{\alpha}\frac{1}{\cos^2\theta} - 4\gamma^2(\frac{\Delta\beta}{\beta})\sin^2\theta \quad (2)$$

where R is the angle dependent reflectivity. The parameters α, β, ρ, γ respectively are the average p-wave velocity, s-wave velocity, density and ratio of S-velocity to P-velocity across the interface. The variable θ is the average angle of incidence. Equation (2) may be written in matrix form *Gm=d* where *G* is the linear operator, *m* the unknown parameter vector containing the velocity and density reflectivity $[\Delta\alpha/\alpha, \Delta\beta/\beta, \Delta\rho/\rho]^T$ and *d* the input data vector (offset dependent reflectivity).

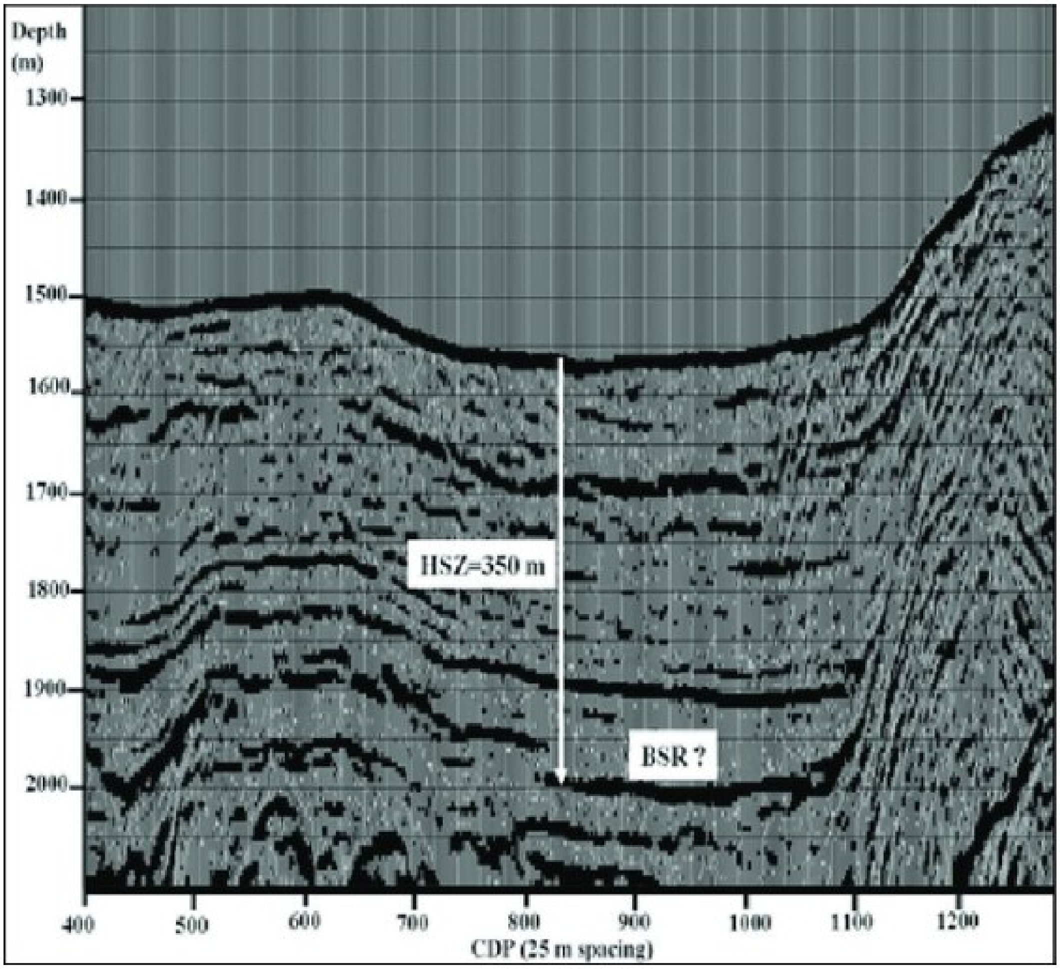

Figure 3: Stacked depth section near the salt dome showing a bright event at the predicted base of hydrate stability zone.

In practice, the inversion of equation (2) is performed using hard constraints to improve the stability of the problem. Xia et al. (2000) use the Gardner equation (Gardner et al., 1974) to remove the density reflectivity and they use the “mudrock relationship” (Castagna et al., 1985) to relate the s-wave velocity to the p-wave velocity.

In this paper, a three parameter least-square inversion is used based on minimizing the following function F:

(3) $$F = \| d - Gm \|^2 + \alpha^2 \| Am \|^2$$

The first term is the data misfit and the second term is the regularization term. This results in equation (4):

(4) $$m = [G^T G + \alpha^2 A^T A]^{-1} G^T d$$

The matrix A of the regularization term is in the form:

(5)

$$A = \begin{bmatrix} 1 & 0 & 0 \\ 0 & a & 0 \\ 0 & 0 & b \end{bmatrix}$$

and the values *a* and *b* are dictated by inversion on synthetic data. In the inversion, the regularization term acts as a weighted minimization of the total energy: $[(\Delta\alpha/\alpha)^2 + (a\ \Delta\beta/\beta)^2 + (b\ \Delta\rho/\rho)^2]$.

The Lagrange multiplier α^2 is determined by minimizing the data misfit.

AVO inversion

The AVO inversion was performed on the unmigrated time section from CDP 1000 to CDP 1120 in the vicinity of the salt tongue as presented on Figure 4. The section contains angles from 0 to 35 degrees assuming straight raypaths. The potential hydrate accumulation is located between 2380 and 2480 ms.

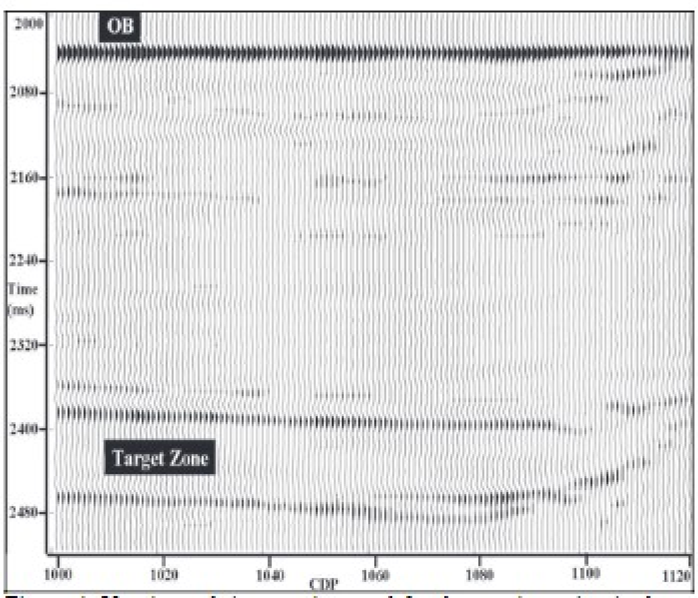

Figure 4: Unmigrated time section used for the avo inversion in the vicinity of the salt dome containing the ocean bottom and the target zone.

Figure 5 shows how the regularization matrix was tuned. First we created a background profile for Vs, Vp and density. The background Vp profile was calculated from the stacking velocity using the Dix equation. The Vs and density profiles were taken from standard models for shallow ocean sediments (Stuart and Caughey, 1977). Next, to explain the reflection events at the target zone, we assumed an hydrate accumulation overlying a free gas reservoir. The Vs, Vp and density profiles were modified from their background values according to published elastic properties of sediments containing hydrates (Dvorkin et al., 1999).

The three parameter least-square inversion was tested on this model The coefficients of matrix A and the lagrange multiplier that minimize the data misfit are:

(6) $a = 0.7$; $b = 1.5$
$\alpha^2 = 0.1$

Using the calibrated matrix A, the constrained least-square inversion is performed on the data shown in figure 4. The final results at CDP 1081 are shown in Figure 6.

We interpret the inverted profiles as follows:
The first reflection event in the target zone corresponds to the top of the hydrate accumulation. The P-wave velocity increases from 1900 m/s to 2400 m/s in the hydrate reservoir. The hydrate accumulation is approximately 40m in thickness and the bottom of the reservoir is located approximately at the predicted base of hydrate stability zone. The transition between hydrate and free gas in the sediment column is gradual. The thickness of the transition layer is approximately 20 m. The bottom of free gas is indicated by the lowest Vp value of 1400 m/s.

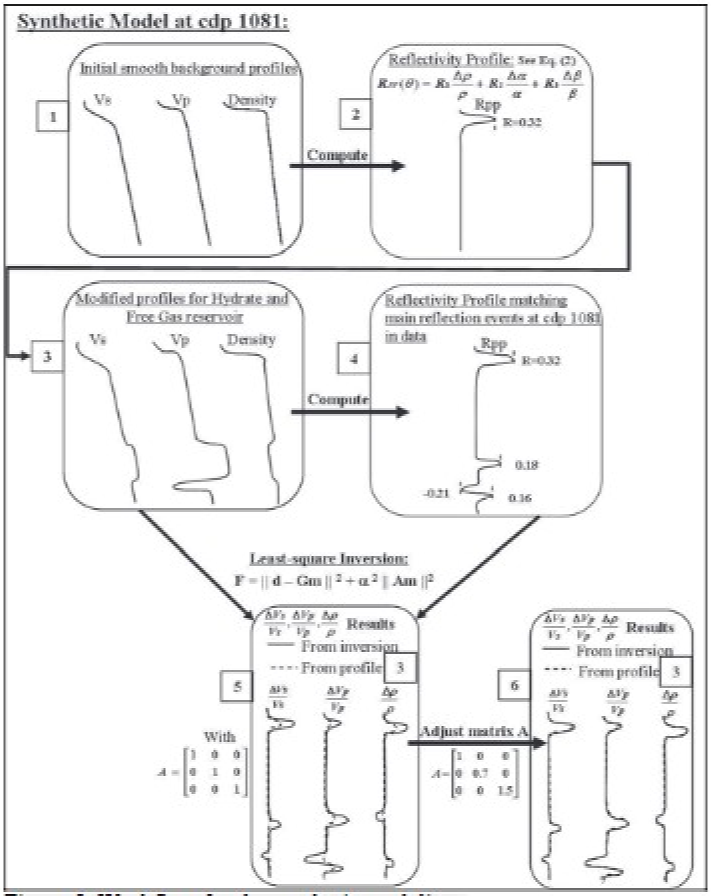

Figure 5: Workflow for the synthetic modeling

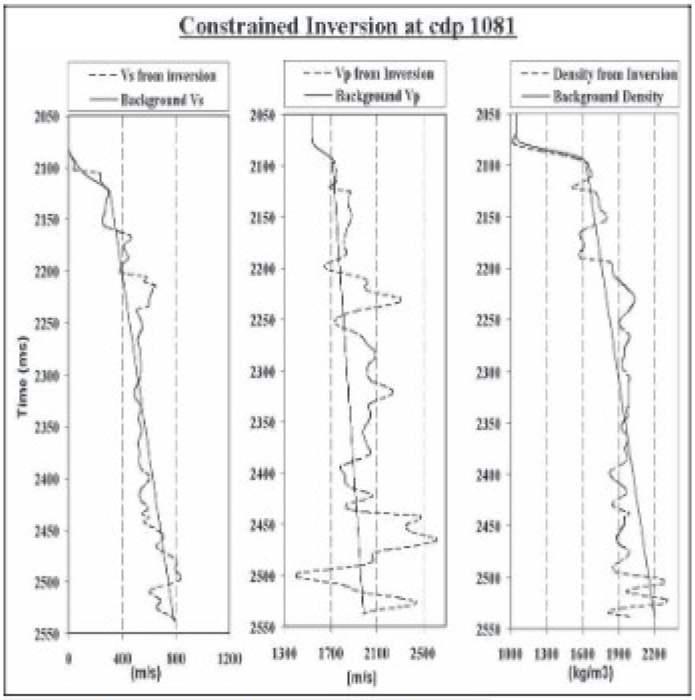

Figure 6: Results of AVO inversion at CDP 1081

To assess the lateral continuity, the Vp profiles at all CDPs are superimposed on the stacked depth section as shown in Figure 7. The hydrate reservoir is continuous from CDP 1000 to 1120 as initially predicted from the seismic section.

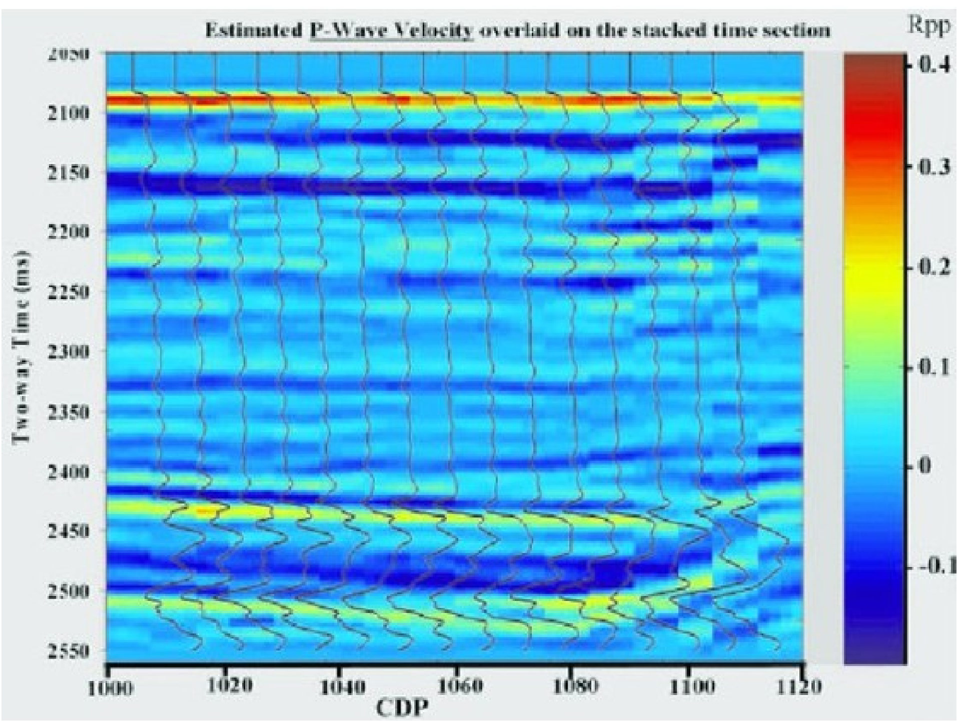

Figure 7: The estimated P-wave velocities at cdp 1000 to 1120 are superimposed on the stacked time section.

Estimation of methane gas volume

The physical properties and elastic models for hydrate bearing sediments were taken from Dvorkin et al. (2000). The model for water saturated sediments is based on the rock physics model of Dvorkin et al. (1999).

In Figure 8, the inverted Vp profile is plotted together with the modeled velocity profile. Figure 8(a) shows modeling results for the hydrate-part-of-the-solid model, while Figure 8(b) uses the hydrate-part-of-the-fluid model. The volume of methane gas is then estimated for 20% to 40% hydrate concentration. The reservoir extends 3000 m from the salt tongue and its thickness is 40 m. The porosity is estimated to 30% at the reservoir depth. The extent of the salt dome in the direction perpendicular to the seismic line is estimated to 3000 m. One unit of hydrate, by volume, contains 164 units of methane gas, by volume. For 20% hydrate concentration, the total volume of methane gas is estimated to 126 billion cubic feet, for 40% concentration, the total volume is 252 billion cubic feet.

Conclusions

A three parameter AVO inversion was applied to selected CDPs along a 2D seismic line collected at Mississippi Canyon Block 383. The constrained AVO inversion was initially calibrated by using a simple forward model containing the main reflection events in the seismic section. The constrained inversion was then performed on the field data and we derived the Vp, Vs and density profiles. At the expected base of hydrate stability zone, a 40 m hydrate accumulation is identified above a 20 m transition between hydrate and free gas. The volume of methane gas in the reservoir is estimated between 124 and 252 billion cubic feet.

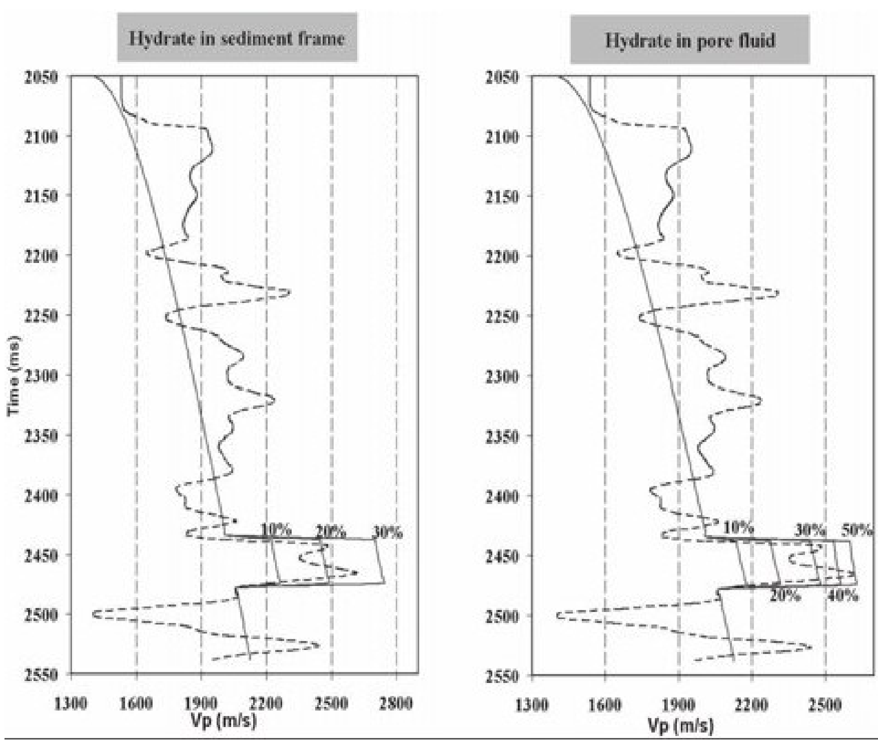

Figure 8: Estimation of hydrate concentration from inverted p-wave velocity profile. Comparison of inverted Vp profile with Dvorkin et al. model results assuming that (a) hydrate is part of the sediment frame (b) hydrate is part of the pore fluid

References

1. Aki, K., and Richards, P.G., 1980, Quantitative seismology: theory and methods: W.H. Freeman and Co.
2. Brown, K.M., Bangs, N.L., Froelich, P.N., and Kvenvolden, K.A., 1996, The nature, distribution and origin of gas hydrate in the Chile Triple junction region, Earth and Planetary Science Letters 139, 471-483.
3. Castagna, J.P., Batzle, M.L., Eastwood, R.L., 1985, Relationships between compressional-wave and shear-wave velocities in clastic silicates rocks: Geophysics, 50, 571-581.
4. Dickens, G.R., and Quinby-Hunt, M.S.,1994, Methane Hydrate Stability in Seawater, Geophysical Research Letters 21, 2115-2118.
5. Dvorkin, J., Helgerud, M.B., Waite, W.F., Kirby, S.H., Nur, A., 2000, Introduction to Physical Properties and Elasticity Models, Natural Gas Hydrate in Oceanic and Permafrost environments, Kluwer Academic Publishers, 245-260.
6. Dvorkin, J., Prasad, M., Sakai, A., and Lavoie, D., 1999, Elasticity of marine sediments, Geophysical Research Letters 26, 1781-1784.
7. Gardner, G.H.F., Gardner, L.W. and Gregory, A.R., 1974, Formation velocity and density – The diagnostic basics for stratigraphic traps: Geophysics, 39, no. 06, 770-780.
8. Sassen, R., Sweet, S.T., Milkov, A.V., DeFreitas, D.A., Kennicutt, M.C., 2001, Stability of Thermogenic Gas Hydrate in the Gulf of Mexico: Constraints on Models of Climate Change, Natural Gas Hydrates: Occurrence, Distribution and Detection, American Geophysical Union, 131-143.
9. Stuart, C.J., and Caughey, C.A., 1977, Seismic facies and sedimentology of terrigenous Pleistocene deposits in Northwest and Central Gulf of Mexico, in Seismic stratigraphy – applications to hydrocarbons exploration, AAPG 26, 249-275.
10. Xia, G., Sen, M.K., and Stoffa, P.L., 2000, Mapping of elastic properties of gas hydrates in the Carolina trough by waveform inversion, Geophysics, 65, no. 03, 735-744.

Acknowledgments

We thank Chevron Texaco for providing the data and financial support for this study. We also thank Jeff Wright and Jorge Mendiguren for helpful discussions.